

# Physical Optics and Field-Strength Predictions for Wireless Systems

James H. (Jim) Whitteker

**Abstract**—Physical optics, or Fresnel–Kirchhoff theory, is often used for studies of particular problems in terrestrial radio-wave propagation. With efficient techniques of numerical integration, it can also be used effectively for routine predictions and for designing terrestrial wireless systems. A computer program of this type has been in use for several years. It is most useful in situations in which the base station (BS) antenna is above local clutter, and over areas large enough that ground cover can be characterized with categories such as “open,” “forest,” “dense residential,” etc., rather than individual buildings. The main calculation is a marching algorithm that simulates diffraction over all the variations in terrain height along radials from the BS. A secondary calculation estimates the additional attenuation due to buildings and trees close to the mobile antenna. This part of the calculation is based on several parameters characterizing the local environment of the mobile antenna. Calculations are slow compared to many traditional methods, but are fast enough for routine use on a PC.

**Index Terms**—land mobile radio propagation factors, physical optics, radio propagation, radio propagation terrain factors, ultrahigh frequency radio propagation terrain factors.

## I. INTRODUCTION

THIS PAPER describes methods implemented in a computer program for predicting signal strength over paths that may be obstructed by irregular terrain and buildings or forest (ground clutter). The most common application is the planning of new wireless systems that operate over distances greater than about 1 km. The program, known as CRC-Predict, was developed for the most part at the Communications Research Centre, Ottawa, Canada, and development continues at Marconi. A previous account [1] is for the most part superseded by the present one. Predictions are based on a detailed simulation of diffraction over terrain (including clutter), and then an estimate of local clutter attenuation. The frequency range of interest is very high frequency (VHF) and ultrahigh frequency (UHF), but there are no definite limits, and the calculations have been compared with measurements up to about 2500 MHz. The algorithm becomes less useful below 30 MHz, because neither the sky wave nor the surface wave is taken into account. At 3 GHz and above, the main limitation in accuracy is that the Fresnel zone becomes small, and uncertainties in ground height and clutter height cause errors of increasing size as the frequency increases. However, the physics of propagation does not change until about 10 GHz, where rain attenuation begins to be significant.

Manuscript received March 14, 2001; revised September 14, 2001.  
The author is with Marconi, Wireless Network Planning, Kanata, ON, K2K 3G7 Canada (e-mail: jim.whitteker@marconi.com).  
Publisher Item Identifier S 0733-8716(02)03293-6.

## II. THEORY OF DIFFRACTION OVER TERRAIN

### A. Physical Optics and Huygens' Principle

The detailed diffraction calculation is based on physical optics, or Kirchhoff theory [2], [3]. The theory may be expressed in terms of the well-known Huygens' principle of physical optics, which states that points in space where there is a wave field may be considered to be elementary sources of radiation, proportional in amplitude to the amplitude of the field. In its most elementary form, physical optics is best known as an intuitive way of solving the problem of diffraction over a single knife edge. Some traditional methods of field-strength prediction are based on this solution repeated for one to three obstacles, assumed to behave as knife edges. Physical optics has been widely used for special studies related to terrain diffraction, particularly when the terrain or the buildings on it can be modeled as knife edges, e.g., [4] and papers cited, therein, or when individual buildings are modeled [5]–[8]. A well-known series due to Vogler [9] is also derivable by physical optics. Physical optics is not so commonly used in a detailed way for routine predictions, because of the time-consuming numerical integration that is required to solve realistic problems. However, an efficient method of numerical integration [10] permits this to be done.

### B. Marching Algorithm

The calculation is based on a path profile, that is, ground elevation as a function of distance from a transmitter. To limit consideration of the terrain to a profile along the great circle path is a simplification of reality, but one that is commonly made, and usually justifiable on the basis of the small size of the first Fresnel zone in the direction perpendicular to the nominal propagation path in comparison with the horizontal extent of geographical features. A path profile is specified as a series of elevations at distances  $x_0, x_1, x_2, \dots$ , from the transmitter, assumed to be joined by straight lines, as indicated in Fig. 1. These elevations are modified by introducing an earth curvature, and allowing for surface cover, as described later. It is not necessary to identify or model terrain obstacles, or to define effective antenna heights. The field is first evaluated, by an elementary calculation, as a function of height at  $x_1$ . That is, the field is just the sum of fields due to a direct (free-space) wave and a wave reflected from a locally plane earth.

### C. Huygens' Principle Without Ground Reflection

The field can be calculated at any height at distance  $x_2$  by the use of Huygens' principle. That is, each point above the ground at distance  $x_1$  is regarded as a source of radiation, and

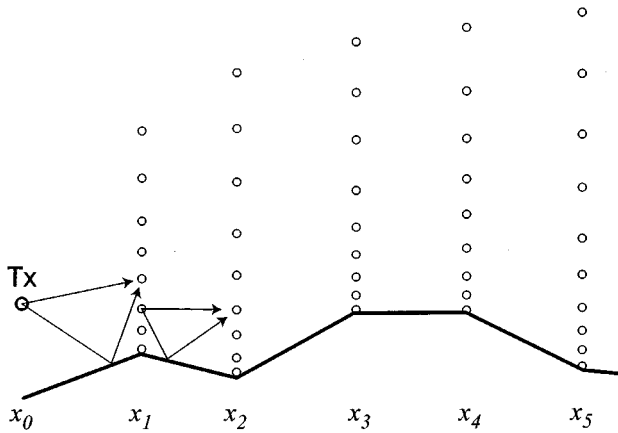


Fig. 1. A terrain profile is specified at points  $x_0, x_1, x_2, \dots$ . A transmitting antenna is indicated by a circle at  $x_0$ , and the field is calculated as a function of height at  $x_1, x_2, x_3, \dots$ , at points schematically indicated by circles.

each contributes to the field at  $x_2$ . Since the field distribution at  $x_1$  is continuous, summing the contributions to the field at  $(x_2, z_2)$  from all the Huygens sources, neglecting the ground for the moment, takes the form of the integral

$$E(x_2, z_2) = \sqrt{\frac{kx_1}{2\pi i(x_2 - x_1)}} \int_{h_1}^{\infty} E(x_1, z_1) e^{ikr} dz_1 \quad (1)$$

where  $k = 2\pi/\lambda$  is the propagation constant, and  $r$  is the distance from  $(x_1, z_1)$  to  $(x_2, z_2)$ . (The transverse horizontal coordinate  $y$  does not appear in (1), since integration over  $y$  has already been done analytically under the assumption of uniformity perpendicular to the propagation direction on the scale of a Fresnel zone, as discussed in [2]). This procedure can be continued to calculate the field as a function of height at  $x_3$  and so on. In the first step in which (1) is applied, where  $E(x_1, z_1)$  is the field due to a point source, (1) becomes the well-known Fresnel integral, but as the marching algorithm proceeds, this is not so, and a numerical integration is required.

#### D. Ground Reflection

It would be possible to take the presence of the ground into account by integrating over Huygens sources at the surface of the ground. However, the simpler alternative has been adopted of integrating again over  $z_1$ , but for a ground-reflected wave. As pointed out in [2], image theory implies that this alternative is exact for perfectly reflecting ground, and is a good approximation for ground that reflects well. This requires only a slight modification to (1), resulting in

$$E(x_2, z_2) = \sqrt{\frac{kx_1}{2\pi i(x_2 - x_1)}} \times \left[ \int_{h_1}^{\infty} E(x_1, z_1) e^{ikr} dz_1 + \int_{h_1}^{\infty} E(x_1, z_1) R e^{ikr_R} dz_1 \right] \quad (2)$$

where  $r_R$  is the length of the reflected path, and  $R$  is the reflection coefficient of the ground. The calculation by (2) of the

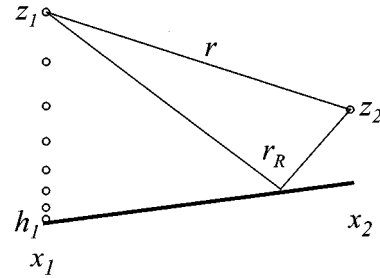


Fig. 2. Integration over  $z_1$  to calculate the field at  $(x_2, z_2)$ .

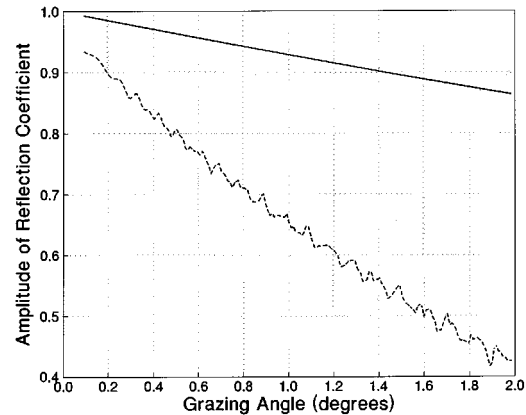


Fig. 3. The amplitude of the Fresnel reflection coefficient for 900 MHz (vertical polarization) for very dry ground ( $\epsilon = 3.0, \sigma = 0.0001$ ) is indicated by the solid line. The broken line indicates the corresponding “reflection coefficient” for a uniform array of knife edges spaced 50 m apart, extending over 2 km (39 edges), with a receiving antenna 3 m above the plane of the edges.

field at a particular point is illustrated in Fig. 2. The integrals are those specified in (27) of [2].

#### E. Ground and Clutter Reflection

For propagation over bare earth, the reflection coefficient can be obtained from standard formulas. However, it is not obvious that these formulas apply to the interaction of the wave with the tops of buildings (or trees). An alternative is to replace the factor  $R e^{ikr_R}$  with a more general function that gives the field at  $(x_2, z_2)$  due to knife-edge scattering of radiation from a point source at  $(x_1, z_1)$ . Such functions can be evaluated numerically [4], [11], although the calculations are time consuming. It turns out that when there are many buildings of uniform height along the path, knife-edge representations of building-tops scatter waves in a coherent way that resembles reflection, but the “reflection” is weaker than for ordinary ground. An example is given in Fig. 3. This resemblance is fortunate, because most simulations done by many methods over the years have not distinguished between cluttered ground and bare ground. It is also fortunate that at UHF, the predicted field strength is insensitive to the ground constants assumed. Preliminary indications are that replacing the standard Fresnel reflection coefficient with approximate reflection coefficients obtained from knife edge in built-up areas does not change the predicted field strength very much, although knife-edge coefficients seem more appropriate.

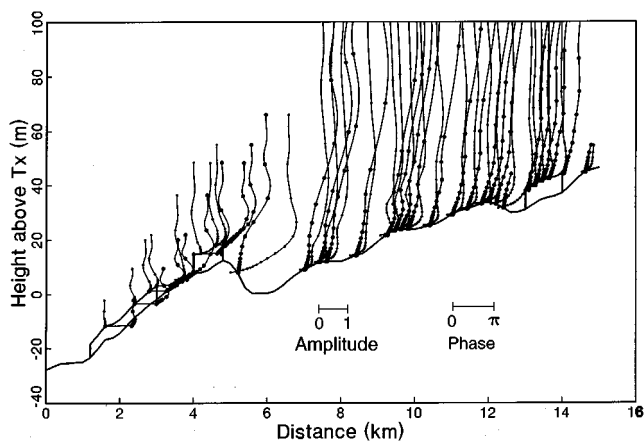


Fig. 4. Points at which the field is calculated for 910 MHz along a radial road near Ottawa. The transmitting antenna is at the origin. Although the field points are physically located in vertical columns, the two sets of points that are shown rising above each point on the ground indicate by their horizontal displacement the amplitude (larger symbols) and phase (smaller symbols) of the wave, both with respect to free-space values.

### III. IMPLEMENTATION—FIELD POINTS

The computation time of the program depends roughly linearly on the number of distances  $x_j$  at which the field is calculated as a function of height, and roughly quadratically on the number of points in the vertical array at each  $x_j$  (because the field must be calculated this number of times, and also the number of steps in each integration depends on this number). The penalty for placing the  $x_j$  too far apart is that the intervening terrain may not be well represented. (If the terrain is smooth, there is a wide range of distances between successive  $x_j$  for which the results do not change.) At the other extreme, if the  $x_j$  are so close together that there are many hundreds of successive integrations, accuracy can begin to fall off from accumulated errors. The penalty for placing the  $z_j$  too far apart is that the field between adjacent points may not be well represented.

#### A. Horizontal Spacing of Field-as-Function-of-Height

As described so far, the wave field is calculated at many heights above every point in the terrain profile. However, for routine calculations, in order to reduce computation time, the field is only calculated as a function of height above the highest terrain, as illustrated in Fig. 4. The procedure for selecting the locations is to trace roughly-estimated wave-normals (or rays) from the transmitter along the radial to the receiving-antenna positions. These rays touch the highest terrain, but pass above lower terrain. The program omits calculating field-as-a-function-of-height on low sections of terrain over which the ray has Fresnel-zone clearance.

This introduces the problem of how to calculate the field due to the wave reflected by terrain that is not populated by field-as-function-of-height, and which in general is not flat. The method adopted is to approximate the nonflat terrain as one or two surfaces with constant curvature, which have well-known reflective properties. The choice of the most significant part of the reflecting surface is based on minimum phase considerations. How exactly to do this is somewhat arbitrary; the method

used here is described in [12]. An expression for a reflection coefficient for a surface that is both curved and rough is given by [13]. This treatment of low-lying ground represents a retreat from the original ideal of not having to fit curves to terrain (not having to model obstacles). However, on obstructed paths, the terrain lying between two hills in a propagation path is likely to have only a minor effect on the field at the end of the path. Therefore, a rough estimate of the reflected field is adequate.

The field amplitude is nevertheless calculated at the mobile antenna height at all the terrain points, with a spacing comparable to the cell size of the elevation grid, which is often 30 m.

#### B. Vertical Spacing of Field Points

Field points are placed close together close to the ground because variations are usually of most interest there. Higher up, it matters less if all the variations are represented, and of course, the calculation of the field must terminate at some height.

The vertical spacing of points that was adopted is as follows: the points just above the ground are spaced so that the phase difference between the incident wave and the wave reflected from nearby ground changes by about 0.1 radians between adjacent points. The highest points, which are high enough to be illuminated by the transmitter, are spaced so that the phase difference between the direct wave from the transmitter and the wave reflected from terrain are quantities of order unity. Between these extremes, the spacing between points follows a geometric progression, except that shadow boundary widths are estimated in order to ensure that transition regions are adequately sampled.

At a great enough height, the vertical variation in the field must be assumed simple enough that the numerical integration can be continued to infinity. Because of this, steep reflections from the ground are artificially attenuated if the resulting interference fringes would be more closely spaced than the field points.

#### C. BS Antenna Pattern

It would be possible to impose the BS antenna pattern onto the field as a function of height at  $x_1$ , and in principle this would be the best way to take it into account. At the present time, however, the simpler alternative is adopted of performing the main calculation for an isotropic transmitter, and adding the antenna pattern later for each position of the mobile antenna. If there is a clear line of sight to the mobile antenna, its position defines the elevation angle; otherwise, the elevation angle to the horizon is used.

#### D. Calculations Without Buildings or Trees

An example of predictions and measured data along a radial through open (cattle grazing) land is shown in Fig. 5. This terrain is favorable for this kind of prediction, since there are very few buildings or trees. The location is Buffalo Hill, at  $50^\circ 36'N$ ,  $113^\circ 9'W$ , near Calgary. The measurements were made with a narrowband transmission, using nine-element Yagi antennas at both ends of the path, both directed along the road on which the measurements were done. The mobile antenna was mounted on a vehicle, which was stopped at intervals, and a mast moved up

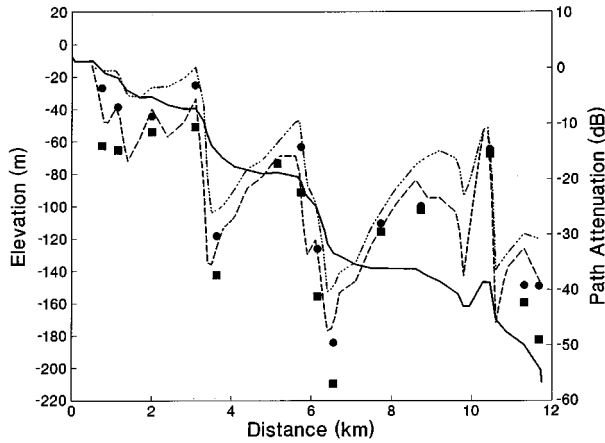


Fig. 5. A terrain profile on open prairie near Calgary, and attenuation with respect to free space 2 m and 8 m above ground, for 910 MHz. The transmitting antenna is located at 0 m (relative) elevation, 7.5 m above ground on the brow of a hill. The square and round symbols represent measured loss at 2 m and 8 m, respectively, and the broken lines represent predicted loss at the same heights.

and down. In this example, most differences between predictions and measurements are within 5 dB, with a few as great as 10 dB.

#### IV. BUILDINGS AND TREES

##### A. Data and Assumptions

Since the demand for most wireless services is in populated areas, and since most services are required at street level, or perhaps on the sides of buildings, the presence of buildings must be taken into account in some way. Trees are often also present, either as forest or individually. It is not assumed that the location or size of individual buildings or trees is known. Rather, use is made of commonly available land-use categories (agricultural, residential, etc.). A typical height of buildings must usually be assigned from assumptions about the category (e.g., suburban houses are one or two stories), and some assumption must also be made about a typical distance between buildings.

##### B. Diffraction Calculation in the Presence of Clutter

In built-up or forested areas, the assumed heights of buildings or trees are added to the terrain height and treated as terrain, and the wave field at the top of the clutter is calculated. These values are then used to estimate the field amplitude at street level, with a simple diffraction calculation, as illustrated in Fig. 6. The calculated field amplitude at street level depends on the rooftop field, the angle of incidence on the roof, and a typical distance from the last rooftop that the wave must pass over to the receiving antenna. This part of the calculation is similar to other models, e.g., [14]–[16].

##### C. Field Amplitude at Street Level

The estimate of field amplitude at street level in cluttered areas can be made a little more realistic than single knife-edge diffraction by considering three contributions to the field, two of which are illustrated in Fig. 6. The first contribution is diffraction over an obstructing building, as already mentioned.

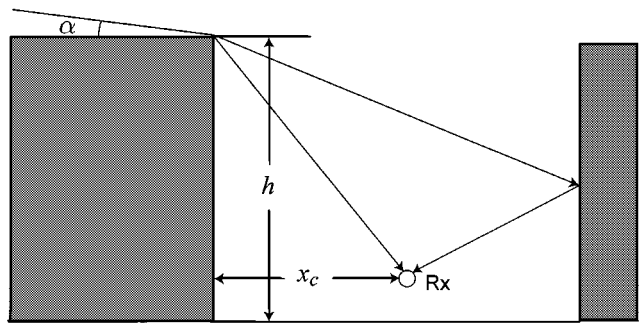


Fig. 6. Calculation of the field strength at street level starting from the field strength at canopy level and angle of incidence. The symbol  $\alpha$  indicates the angle of incidence, estimated geometrically from the height of previous clutter or terrain,  $h$  indicates the height of buildings locally, and  $x_c$  indicates an assumed distance from the nearest clutter that the wave must pass over to the receiving antenna.

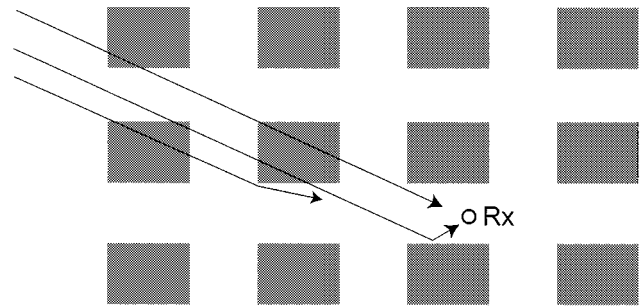


Fig. 7. Top view of a possible scenario for diffraction over buildings to a receiving antenna Rx. The wave arriving at the receiving antenna has often not passed over the nearest building, but over a building farther away.

The second contribution is a reflection back from the next row of buildings, which fills in the shadow from the obstructing building somewhat, and changes the vertical field distribution. An effective reflection coefficient for this must be assumed, which should usually be less than the reflection coefficient of a building wall, since there are usually spaces between buildings, as illustrated in Fig. 7.

The third is a contribution due to waves infiltrating horizontally along streets and around buildings. This contribution is introduced as a knife-edge horizontal diffraction around a building of some assumed width. This is a great simplification of reality, but at least it prevents the attenuation from growing unreasonably as clutter height becomes greater, and results in a small vertical field gradient at street level in the urban core, a behavior shown by measurements.

##### D. Clutter Parameters

The clutter environment is characterized by a few parameters: the typical height of buildings or trees (usually buildings), some indication of density, and a value for absorption due to individual trees and perhaps other absorbers. Height is known or assumed. The characterization of building density is a distance  $x_c$  for diffraction down to street level from the last obstructing building. It is chosen to be somewhat greater than half the street width or road allowance, because propagation is not perpendicular to the street in general. Also, because there are gaps between buildings, the obstructing building may not even be on the same street. The value  $x_c = 50$  m is commonly adopted. The

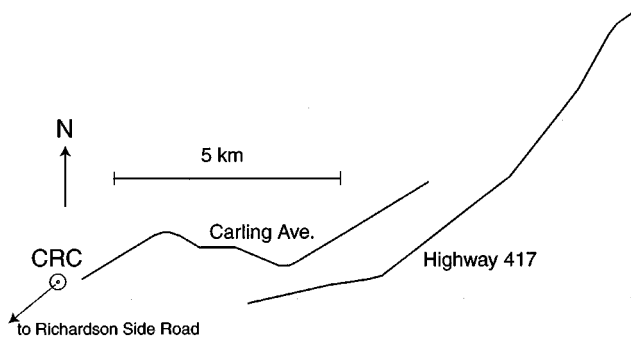


Fig. 8. The Communications Research Centre site and the three drive-test routes used for illustration.

absorption is often set to zero initially and reset in the process of drive-test tuning.

Although an attempt has been made to make it somewhat realistic, the physical model of transmission down to street level is still much simpler than reality. Because of this, and because the size and distribution of buildings is usually not known in detail, the choice of values for the parameters are somewhat arbitrary, and are made with the general guidance of comparisons between predictions and measurements.

V. CALCULATIONS AND DRIVE TESTS IN CLUTTERED AREAS

Three test-drive routes in the Ottawa area are indicated in Fig. 8. The transmitter site, Communications Research Centre, lies in a green area west of Ottawa. The 910 MHz signal for Richardson Side Road was a narrowband signal transmitted from an omni-directional vertically polarized antenna 27.8 m above ground. For the other routes, digital audio broadcast signals at 1.5 GHz were transmitted from an omni-directional vertically polarized antenna 27 m above ground. Reception was with an omni-directional antenna mounted on the roof of a van.

A. Richardson Side Road: Open, Suburban, Some Trees

Richardson Side Road lies almost on a (straight-line) radial from Communications Research Centre, beginning at about 2 km away. The path passes partly through a residential area and small woodlots but mostly through open farmland, as shown in Fig. 9. For this example, the terrain surface-cover data were obtained in part by on-site inspection. For the most part, the predictions are within 10 dB of measurements, but near trees and buildings the difference is 15 dB in places. In suburban and wooded areas, the signal strength on a precisely radial road may be expected to be greater than on a road with a more general orientation, because the radio wave is channeled along the open area created by the road. Therefore, while a radial road is convenient for making calculations and displaying the results, it is not ideal for checking predictions in built-up or wooded areas.

B. Carling Avenue: Residential With Clear Areas

Carling Avenue is the road leading into Ottawa from Communications Research Centre. In contrast to the last example, the open areas indicated in Fig. 10 are mostly not farmland. There are numerous trees along the road and scattered here and there.

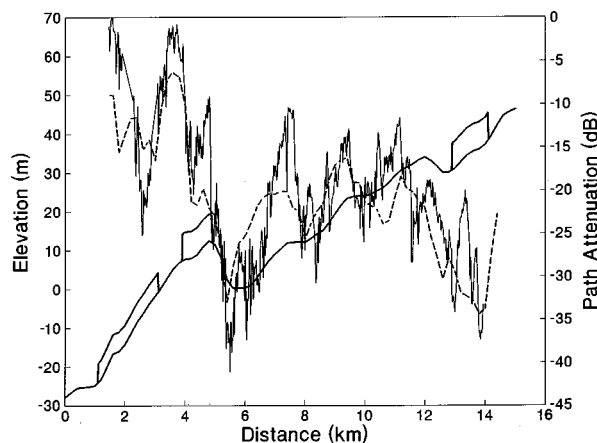


Fig. 9. Predicted and measured field strength with respect to free-space field strength at 910 MHz along Richardson Side Road. The transmitting antenna is at the origin. The rising solid line represents ground elevation, while the block-shaped objects on the ground represent, at about 2 km, residential buildings, and at about 5 and 14 km, forested areas. The broken line represents predicted path loss (with respect to free-space path loss), and the solid line represents measured path loss, recorded every 2 m, but plotted here as 20-m medians.

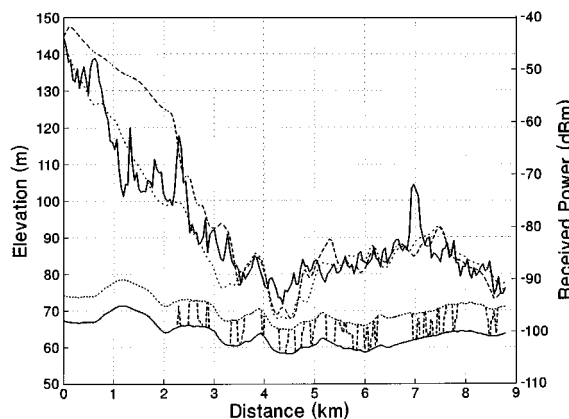


Fig. 10. Ground elevation with areas of buildings and trees (mostly buildings) indicated (lower part of graph) along with measured (solid line) and calculated (broken line) received power levels at 1500 MHz along Carling Avenue. The mobile receiver goes from 1.5 to 8.5 km from the transmitter. The land-cover is mostly residential, with open areas, as indicated by a broken line that makes transitions from ground to canopy that are not perfectly sharp because values were interpolated from a grid. An additional curve (dotted) above the ground and another (also dotted) for received power indicates the result if the “open” area, which contains trees in many places, is considered as cluttered rather than “open”.

That is, the “open” areas are in fact somewhat cluttered. The diagram shows the prediction under the assumption that the open areas really are open, and also under the assumption that they are cluttered. In this case, the prediction is clearly better if they are assumed to be cluttered. A similar result can be obtained by assigning an additional attenuation to “open” areas. The difficulty is that other “open” areas in the same service area really are open, such as the farm land of Fig. 9. This contrast illustrates a limitation of most land-use data: a single category can contain substantial physical differences. Apart from this consideration, the agreement between predictions and measurements on this route is very good.

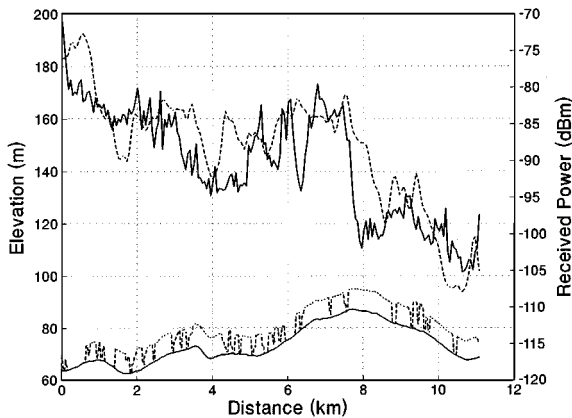


Fig. 11. Ground elevation with buildings and trees indicated (lower part of graph) along with measured (solid line) and calculated (broken line) received power levels at 1500 MHz along Highway 417 east of the Communications Research Centre in Ottawa. The transmitter is at Communications Research Centre, 27 m above ground. The mobile receiver goes from 4.1 to 13.9 km from the transmitter. The land-cover is mostly residential, with a few open areas, as indicated.

### C. Highway 417: Mostly Residential With Small Clearings

Highway 417 is a major motorway that passes through the city. Results are shown in Fig. 11. This route is almost entirely built up, with only small clear areas. The agreement between predictions and measurements is not quite as good as in the previous example. Over distances of a kilometer or more, the two curves correspond fairly well, but not everywhere over smaller distances. This may be due in part to limitations in the calculation, but certainly it is at least partly due to limitations in the terrain data.

## VI. ADDITIONAL CALCULATIONS

### A. Tropospheric Scatter

The path loss due to tropospheric scatter propagation is calculated along with the diffraction calculation, using standard methods [17]. This mode of propagation is usually important only on very long paths, say over 50 or 100 km, on which the diffracted field is very small.

### B. Time Variability

Field-strength variations due to atmospheric effects become significant for paths greater than about 50 km, and an estimate may be required of the signal exceeded for various percentages of time. The empirical curves of [17] are used. This feature is usually of interest only in estimates of interference from distant sources.

### C. Location Variability

For mobile terminals close to the ground, the observed signal strength is subject to fast fading due to multipath interference and due to shadowing by objects such as individual buildings and trees that are too small to be included in the kind of terrain data under consideration here. Furthermore, the error in predicting the median signal strength for a given small area

has a distribution that must be taken into account in any estimate of the probability that the signal exceeds some value. In CRC-Predict, which does not consider fast fading, an estimate of location variability due to shadowing variations is based mostly on measurements made in eastern Canada. The frequency dependence follows Okumura *et al.* [18]. The distribution is assumed to be log-normal, making it easy to combine the location variability with an assumed log-normal prediction error, to arrive at a standard deviation of location variability of prediction error. This commonly turns out to be 7 or 8 dB. System planners can either use the estimate provided by the program, or use their own experience to set power margins. If drive tests are available, the statistics of the difference between measurements and predictions can serve as guide.

### D. Drive-Test Tuning

For completely bare terrain, no tuning is needed. Given terrain elevations (and electrical constants, which are usually not important at UHF and above), the prediction is completely deterministic. With realistic building heights, untuned predictions in cluttered terrain are usually also reasonably good. However, for cluttered terrain, tuning the model so that mean predicted field strengths from predictions and measurements agree is usually beneficial, mostly due to the fact that the environment is often not well known.

Ideally, the typical height of buildings is not an object of tuning, but is known from data. However, if building heights are not known, they may be adjusted in a tuning process. The most direct and easiest method of tuning is to adjust a parameter that is intended to take into account local absorption due to individual trees and other unknown factors, but which is expressed in decibels, and can be used simply as a correction factor.

## VII. PREDICTION ERROR

Measurements made in areas where the ground is undulating, but where there is no clutter, indicate that the standard deviation of prediction error is about 5 dB in such places. However, in most areas of practical interest, the standard deviation of prediction error is greater than this, 6–9 dB being typical.

The accuracy of predictions depends greatly on the accuracy of the terrain data, including clutter data. The apparent prediction error can also depend on the accuracy of the location determination of measurements, which sometimes are made close to clutter-type boundaries. Land use does not always correspond well to radio transmission characteristics. For example, there is a great difference between a residential area containing three-story houses and mature trees and one containing one-story houses and shrubs. “Commercial/Industrial” says more about what people do there than what structures might impede radio waves. A variation in “open” areas has already been mentioned.

In areas with steep slopes, off-path scatter can be significant. CRC-Predict does not at present take this into account, although backscatter is estimated. Therefore, predicted field strengths can be too low in places that are in deep shadow along the nominal path, but close to an illuminated slope off path. A complete three-dimensional (3-D) diffraction calculation of the kind

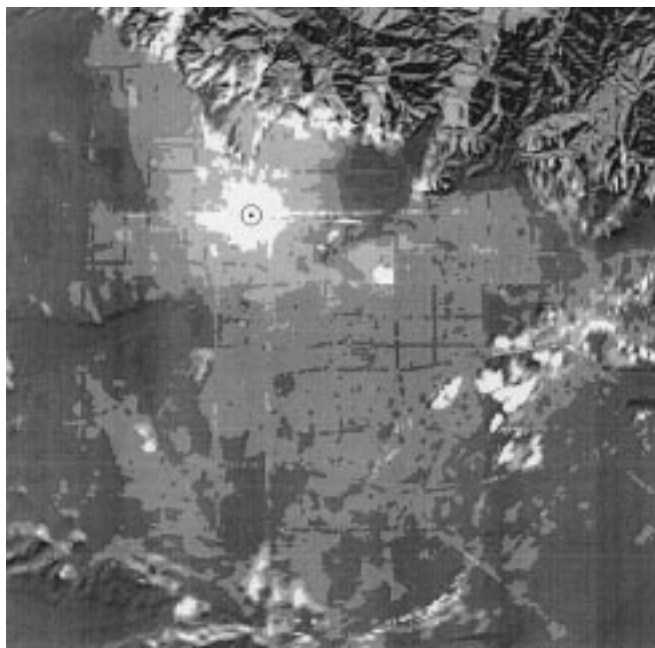


Fig. 12. A coverage plot for part of a code division multiple access (CDMA) system near Los Angeles. At the top and bottom of the diagram, the shading indicates the mountainous topography. In the rest of the diagram, which is in a valley, the shading indicates predicted field strength. The valley is not entirely flat, but has much less relief than the mountains. Most of the coverage area is residential or commercial/industrial. The omni-directional transmitting antenna is indicated by a point and circle. The roughly rectangular grid that is visible in some places represents field strength measured along roads, with the same shading as the predicted field strength. Where the two field strengths lie in the same interval of 10 dB, the drive-test routes are invisible, but are visible where the field strengths lie in different intervals.

described above would be too time consuming, but some 3-D features can be added by a search of steep illuminated terrain, e.g., [19], [20] and such an addition is planned.

## VIII. AREA COVERAGE AND APPLICATIONS

### A. Area Coverage

An example of an area-coverage prediction is shown in Fig. 12. Here a grey scale is used to represent field strength. The picture was obtained from commercial RF planning software that usually represents signal levels with a color code. For system planning, this is the sort of representation that is usually used, rather than the cross sections shown in preceding diagrams. In a complete system, there would be many base stations (BSs), with corresponding coverage patterns, and system performance calculations that are based on the predicted field-strength values. The results of measurements are also indicated in the diagram. In most places measurements and predictions agree well. One limitation of this kind of calculation is illustrated in the road that lies on a radial directly east from the transmitter, where the signal level is substantially higher than calculated. This limitation can sometimes be overcome by including the road in the clutter data as an open area, provided the road is wide, and the clutter data are not too coarse.

As an example of computation time, a 10-km-radius coverage calculation, using 180 radials on 30-m terrain data, takes between one and two minutes, depending on terrain irregularity,

on a personal computer with a Pentium III processor running at 450 MHz.

### B. Applications

The algorithm is intended for coverage and interference calculations over large enough distances that the coverage is not dominated by the distribution of individual buildings, and in which the BS antenna is above nearby buildings or other clutter. It has been applied to planning broadcast, mobile services, and cellular telephone systems including their modern derivatives. The range of applications depends more on the planning software in which it is embedded than on the prediction algorithm itself.

In its present form, it is intended to be used with terrain data that includes clutter information with a pixel size of about 30 m or larger. (30 m is commonly used.) With much smaller pixel sizes, the area covered by a land-use category can become comparable with the size of a single building. High-resolution terrain data including individual buildings are increasingly becoming available, and may be used with the program in the future, although the operation will have to be somewhat different, since most of the clutter parameters will lose their meaning.

## IX. SUMMARY AND CONCLUSION

New wireless systems require accurate field-strength predictions that make full use of detailed terrain and clutter data. The Physical-Optics diffraction calculation described here takes terrain elevation into account in a detailed way. However, it uses commonly available classifications of ground cover rather than data on individual buildings. The calculation is physically based, using approximations to the wave equation that are appropriate for terrestrial radio-wave propagation. It is comparable in some ways to the Parabolic Wave Equation Method [21], [22], although it cannot take atmospheric structure into account (except for the usual 4/3 earth correction) and is based on integration rather than a differential equation. Another method based on integration is the Integral Equation Method [23], which, however, integrates over the ground. The calculations are slow compared to more traditional methods that do not require repeated integration. Nevertheless, on a modern PC, a full-circle area-coverage calculation takes only a few minutes, depending on the area, and it is practical to use it to design extensive systems with the benefit of accurate and detailed field-strength estimates.

## ACKNOWLEDGMENT

The author would like to thank two groups at the Communications Research Centre for the digital radio measurements in the Ottawa area: B. McLarnon, project leader for the transmitter, R. Voyer, research manager for the field-strength measurements, and F. Gautier for designing the measurement system; and F. Gautier, T. Kahwa, and R. Matsunaga who performed the measurements. The author would also like to thank R. Charron for the Calgary measurements, and N. Reed for the R. Road measurements.

## REFERENCES

- [1] J. H. Whitteker, "The CRC VHF/UHF propagation prediction program," in *Proc. Beyond Line-of-Sight Conf. (BLOS)*, Texas, Austin, Aug. 2–4, 1994, Paper 6.
- [2] —, "Fresnel–Kirchhoff theory applied to terrain diffraction problems," *Radio Sci.*, vol. 25, pp. 837–851, Sept.–Oct. 1990.
- [3] —, "Physical optics and terrain diffraction," *The Radioscientist Bulletin*, vol. 5, pp. 111–116, Sept. 1994.
- [4] L. Piazzzi and H. L. Bertoni, "Effect of terrain on path loss in urban environments for wireless applications," *IEEE Trans. Antennas Propagat.*, vol. 46, pp. 1138–1147, Aug. 1998.
- [5] C. J. Haslett, "Modeling and measurements of the diffraction of microwaves by buildings," *IEE Proc. Microwave Antennas Propag.*, vol. 141, pp. 397–401, Oct. 1994.
- [6] C. C. Constantinou and L. C. Ong, "Urban radiowave propagation: A 3-D path-integral wave analysis," *IEEE Trans. Antennas Propag.*, vol. 46, no. 2, pp. 211–217, Feb. 1998.
- [7] R. A. Russel, C. W. Bostian, and T. S. Rappaport, "A deterministic approach to predicting microwave diffraction by buildings for microcellular systems," *IEEE Trans. Antennas Propagat.*, vol. 41, pp. 1640–1649, Dec. 1993.
- [8] S. V. Savov, J. H. Whitteker, and R. Vasilev, "Attenuation of waves behind a building," *Proc. Inst. Elect. Eng.—Microwave Antennas Propagat.*, vol. 146, pp. 145–149, Apr. 1999.
- [9] L. E. Vogler, "An attenuation function for multiple knife-edge diffraction," *Radio Sci.*, vol. 17, pp. 1541–1546, Nov.–Dec. 1982.
- [10] J. H. Whitteker, "Numerical evaluation of one-dimensional diffraction integrals," *IEEE Trans. Antennas Propagat.*, vol. 45, pp. 1058–1061, June 1997.
- [11] —, "A generalized solution for diffraction over a uniform array of absorbing half-screens," *IEEE Trans. Antennas Propagat.*, vol. 49, pp. 934–938, June 2001.
- [12] —, "Estimating the field reflected from irregular terrain," presented at the 8th Int. Conf. Antennas Propagation, ICAP 93, 1983.
- [13] P. Beckmann and A. Spizzichino, *The Scattering of Electromagnetic Waves from Rough Surfaces*. Norwood, MA: Artech House, 1987, p. 503.
- [14] J. Walfisch and H. L. Bertoni, "A theoretical model of UHF propagation in urban environments," *IEEE Trans. Antennas Propagat.*, vol. 36, pp. 1788–1796, Dec. 1988.
- [15] R. Grosskopf, "Prediction of urban propagation loss," *IEEE Trans. Antennas Propagat.*, vol. 42, pp. 658–665, May 1994.
- [16] L. Juan-Llácer, L. Ramos, and N. Cardona, "Application of some theoretical models for coverage prediction in macrocell urban environments," *IEEE Trans. Veh. Technol.*, vol. 48, pp. 1463–1468, Sept. 1999.
- [17] P. L. Rice, A. G. Longley, K. A. Norton, and A. P. Barsis, "Transmission Loss Predictions for Tropospheric Communications Circuits," National Bureau of Standards Technical Note 101, Boulder, CO, NTIS AD-687 820, 1967.
- [18] Y. Okumura, E. Ohmori, T. Kawano, and K. Fukuda, "Field strength and its variability in VHF and UHF land-mobile service," *Rev. Electr. Commun. Lab.*, vol. 16, pp. 825–873, Sept.–Oct. 1968.
- [19] T. Kürner, D. J. Cichon, and W. Wiesbeck, "Concepts and results for 3D digital terrain-based wave propagation models: An overview," *IEEE J. Select. Areas Commun.*, vol. 11, pp. 1002–1012, Sept. 1993.
- [20] P. F. Driessen, "Prediction of multipath delay profiles in mountainous terrain," *IEEE J. Select. Areas Commun.*, vol. 18, Mar. 2000.
- [21] M. Levy, *Parabolic Equation Methods for Electromagnetic Wave Propagation*. Stevenage, U.K.: IEE, 2000, p. 353.
- [22] D. J. Donahue and J. R. Kuttler, "Propagation modeling over terrain using the parabolic wave equation," *IEEE Trans. Antennas Propagat.*, vol. 48, pp. 260–277, Feb. 2000.
- [23] F. K. Akorli and E. Costa, "An efficient solution of an integral equation applicable to simulation of propagation along irregular terrain," *IEEE Trans. Antennas Propagat.*, vol. 49, pp. 1033–1036, July 2001.



**James H. (Jim) Whitteker** received the B.Sc. degree from Carleton University, Ottawa, in 1962, and the Ph.D. degree in physics from the University of British Columbia, in 1967. He was a postdoctoral fellow at University College London in 1967–1969, working in atomic collisions.

He worked at the Communications Research Centre in Ottawa from 1969 to 1999. For the first ten years, his work was on the structure and dynamics of the polar topside ionosphere. For the next 20 years, he worked on VHF and UHF terrestrial radio-wave propagation, and on related topics including topographic data. In 1999, he joined Northwood Technologies, which is now part of Marconi, to do research and development in radio-wave propagation. His particular interest is the use of physical-optics techniques for calculating diffraction attenuation due to terrain obstructions.